Journal of Materials Chemistry

Cite this: *J. Mater. Chem.*, 2011, **21**, 14135

www.rsc.org/materials

FEATURE ARTICLE

Fabrication of nanostructures using polymer brushes

Sara V. Orski, Kristen H. Fries, S. Kyle Sontag and Jason Locklin*

Received 10th March 2011, Accepted 4th May 2011
DOI: 10.1039/c1jm11039j

Polymer brushes offer a surface platform consisting of densely packed macromolecular monolayers that can be used to generate and control nanostructures at surfaces based on the cooperative movement of interacting, stretched polymer chains in response to changes in the surrounding microenvironment. Depending on the chemical composition of the polymer and applied stimuli such as solvation or temperature, interfacial properties of polymer brushes can induce surface topographies that have been used to switch adhesion, morphology, wettability, and surface free energy. This review highlights recent advances in polymer brush fabrication using surface initiated polymerization techniques, with a particular emphasis on the advantages of using brushes to template surface properties at the nanoscale.

Introduction to polymer brush nanostructures

Nanostructured surfaces have recently emerged as important platforms for the development of applied nanotechnology, where the precise control of surface properties can be fabricated on tangible, macroscale substrates. Control of interfacial properties such as wettability, adhesion and self-assembly at the solid-solid, solid-liquid, and solid-air interface is the driving force for new developments in a variety of fields such as sensors, electronics, and biomedical research.[1–3] Interfaces also play a critical role in the development of new materials for nanotechnology, where the understanding of chemistry and physics in these small dimensions present a considerable challenge.[1] In order to develop robust, nanostructured interfaces with tunable properties, surface-bound polymers are a suitable candidate to meet these criteria.[4]

Polymer chain ends that are covalently tethered to a surface with a density high enough to alter the unperturbed solution dimensions of the chains are known as polymer brushes.[5] Films generated from polymer chains in extended conformations exhibit surface phenomena that are different than polymers deposited onto a substrate from solution, such as wetting,

Department of Chemistry and Faculty of Engineering, University of Georgia, Athens, GA, 30602, USA. E-mail: jlocklin@uga.edu; Fax: +(706) 542-3804; Tel: +(706) 542-2359

(from left to right) Jason Locklin, Kristen H. Fries, S. Kyle Sontag, Sara V. Orski

Sara V. Orski (right) is from Centreville, VA and received her B.S. in chemistry (2006) from the College of William and Mary. She is a doctoral candidate in the Locklin group working on functional active ester polymer brushes and orthogonal assembly. Kristen H. Fries (front) is a native of Chesapeake, VA. She received her B.S. in psychology at James Madison University (Harrisonburg, VA) in 2006. She is currently a doctoral candidate under the direction of Dr Jason Locklin specializing in light-responsive polymer brush coatings. S. Kyle Sontag (back) is a native of St. Paul, MN. He received his B.S. in chemistry at Augsburg College (Minneapolis, MN) in 2007. He is currently a doctoral candidate under the direction of Jason Locklin developing new strategies for surface initiated polymerization of conjugated polymers. Jason Locklin (left) obtained both his BS in Chemistry (1999) from Millsaps College and his PhD in Chemistry (2004) at The University of Houston. In 2005, he moved to Stanford University as an Intelligence Community Postdoctoral Fellow and in 2007, he joined the faculty at the University of Georgia as an Assistant Professor in the Department of Chemistry and Faculty of Engineering. He has been awarded the Central Intelligence Agency Young Investigator Award (2007) and the NSF CAREER Award (2010). His group is currently investigating surface-initiated polymerization reactions, orthogonal self-assembly, Kumada-transfer polycondensation, and stimuli-responsive interfaces.

phase-segregation, adsorption of molecules and macromolecules, lubrication, and diffusion control. These unique properties of polymer brushes over other thin polymer films and microgels are dictated by the ordered, extended chains that are perpendicular to the surface. The ordered chains are extended on the densely grafted surface to balance two opposing energies: the entropic energy gained by a random walk configuration of the polymer chains and the energetic favourability of the chains to be highly solvated and non-overlapping.[6] This energy balance determines many physical properties of polymer brushes such as lower compressibility or high stiffness not observed in other polymer thin films. In addition, the extended conformation yields a greater surface area to the polymer thin film. The three dimensional brush allows for greater numbers of functional groups per unit area, allowing the side chain functionality to have greater influence on the interfacial chemistry. In contrast, thin polymer films and microgels are coiled and intercalated at the surface, which causes poor solvation of the overlapping chains and buried functional groups within the film layers. Several recent reviews have been dedicated to topics including the synthesis and applications of polymer brushes in fields like biomaterials, sensors, and nanotechnology.[2,7,8]

The degree to which polymer chains in the brush regime interact with each other to exhibit these surface phenomena is largely determined by their method of formation. Polymer brushes can be formed in a "grafting to" approach by synthesizing a polymer in solution with a reactive functional group at one end of the chain, which is covalently attached to a complimentary functional group on the surface.[9,10] This process, however, is diffusion limited, which keeps polymer brush grafting density low as well as limits the degree of chain extension from the surface. As polymer chains are more likely to be in their entropically favoured random coil configuration in solution, they remain somewhat coiled once attached to the surface, forming a blocking layer to surrounding reaction sites. These non-interacting random coils are referred to as the "mushroom regime" which, in good solvents, have a thickness (H) proportional to their degree of polymerization (N).

Polymer brushes are also synthesized by the direct polymerization from an immobilized initiator species on the surface in a "grafting from" approach.[6,11] Chains that are grown through surface initiated polymerization (SIP) have higher grafting density, σ, which is typically reported in units of chains/nm^2. The distance between grafted polymer chains is typically much less than the size of the polymer coil, or Flory radius.[12] This configuration is known as the "brush regime," where the brush thickness is proportional to $N\sigma^{1/3}$.[11] Due to excluded volume effects, the polymer chain will forcibly grow in a more extended conformation as the polymerization proceeds. While this extended conformation has entropic energy loss, the stretched chains can interact more collectively. In this geometry, selective control of the polymer brush nano-environment, brought about by conformational changes using stimuli such as temperature or polymer solvation, can dramatically alter film properties such as thickness and morphology. These properties are vital, and can be used to generate and control nanostructures.

Polymer brushes that are generated through "living" or controlled polymerization techniques are especially attractive towards the fabrication of nanostructures due to the precise control over molecular weight and low polydispersity. These techniques include, but are not limited to, atom transfer radical polymerization (ATRP), ring opening metathesis polymerization (ROMP), nitroxide mediated polymerization (NMP), and Kumada-type polymerization (KCTP) reactions.[8,13–21] Using living polymerizations adds a further degree of control over surface morphology as the extended polymer chains will have a very small molecular weight distribution, making a more homogenous collective polymer response.

This review article summarizes recent progress in the field of polymer brushes with respect to both templating nanostructures on macroscopic surfaces and using brushes to tune or amplify existing nanostructures. The article focuses on the developments in mixed and block copolymer brushes, polymer brush gradients, stimuli responsive polymers, lithographically ordered polymers, and specialized brushes such as conjugated and multicomponent polymer surfaces.

Mixed polymer brushes

The increasing research interest involving mixed polymer brushes in the last decade has arisen because of the stimuli- responsive nature of these films. The topographical and surface energy changes that occur in these systems are associated with the selective solvation of one of the polymeric chain types tethered to the surface. This has led to the creation of switchable and responsive surface properties such as wettability, surface charge, chemical composition or morphology, and mechanical properties. Experimental studies on mixed brushes began over a decade ago when Sidorenko *et al.* reported the synthesis of mixed homopolymer brushes of polystyrene (PS) and poly(2-vinylpyridine) (P2VP) with brush thicknesses ranging from 10–100 nm, by a two-step conventional free radical polymerization process.[22] This mixed brush exhibited reversible switching properties in response to conformational changes brought about by selective solvation of one of the two polymer components. Since this work, considerable effort has been made in research towards the synthesis, characterization, phase morphologies, and applications of mixed brushes generated using a wide variety of SIP methodologies.[23–39]

In terms of nanostructure generation, several groups have observed reorganization of mixed brushes in response to solvent and pH changes.[10,21,32,33,37,40–53] Santer *et al.* examined the morphology changes of two types of mixed PS-poly(methylmethacrylate) (PMMA) brushes that differed in their modes of attachment to the surface in response to solvent changes,[54,55] while others have investigated the switching mechanism of PS-PMMA mixed brushes.[45] Ionov *et al.* patterned mixed brushes of P2VP and polyisoprene with brush thickness of 5.1 nm using a reversible chemical patterning technique, where the brushes demonstrated switching behaviour in response to different solvents.[51]

The pH responsive behaviour of mixed polyelectrolyte (PE) brushes has been studied for applications involving changes in morphology, wettability, and ion transport to electrodes.[41,56,57] Mikhaylova *et al.* studied the switching behaviour of a stimuli-responsive mixed PE brush containing poly(acrylic acid) and P2VP using infrared spectroscopic ellipsometry (IRSE).[41] The protonation and deprotonation reaction was monitored in

aqueous solutions with pH ranging from 2 to 10, and the structural and chemical changes in the polymer brush layer were identified from the analysis of IRSE. Also, a switchable mixed PE brush of incompatible polymers, poly(dimethylsiloxane) (PDMS) and P2VP, was designed that demonstrates excellent gating properties due to the regulation of ion transport through nanoscopic domains formed by the swelling/shrinking of P2VP chains in response to changes in pH.[57]

Mixed brushes have also been designed so that properties such as nanomechanics or adhesion can also be tuned using external stimuli. LeMieux *et al.* synthesized mixed polymer brushes of two incompatible polymers with brush thicknesses between 20–150 nm that had a nanostructured surface exhibiting microphase segregation, as well as different mechanical properties based on solvent.[58] They have also fabricated stratified polymer surfaces from a poly(n-isopropylacrylamide) (PNIPAM) -containing mixed brush that undergo a change in mechanical response based on temperature.[59]

The switching of adhesive properties in mixed polymer brushes of PS and P2VP have also been observed, where the exposure of the brush to select solvents for PS and P2VP modifies film organization and outer surface composition.[60] Mixed polymer brushes of poly(ethylene glycol) and P2VP have also been designed to act as nanolayers for tunable bacterial adhesion.[61] Lastly, Sheparovych *et al.* described a mixed polymer brush of PDMS and polyethyleneoxide (PEO) with tunable adhesive properties.[62] Atomic force microscopy (AFM) studies show that in water, the swollen PEO chains occupy the topmost layer of the brush, whereas in air, the mixed brush rapidly reorganizes and the PDMS chains constitute the topmost layer. Due to this rapid switching of morphology, the mixed polymer brush has low adhesive properties in both water and air.

Block copolymer brushes

Block copolymer brushes, which undergo nanophase separation due to two immiscible blocks, have also been used to template nanostructured surfaces similar to those observed in mixed polymer brush systems. This was first demonstrated by Zhao and Brittain, who measured the change in surface free energy for poly(styrene-*b*-methyl methacrylate) brushes in good and poor solvents. They observed nanoscale phase separation and a change of contact angle representative of PS and PMMA homopolymers as the brush rearranged in solvents of different polarity.[63] This work has been extended to include the reversible rearrangement of polystyrene and poly(methyl methacrylate-*b*-pentafluorostyrene) in different solvents, measuring the wettability changes that occur upon solvation or brush collapse.[64]

Architectures of nanostructured polymer brushes vary between alternating blocks on a linear polymer brush or arms with Y-shaped architectures, where the two immiscible blocks originate from the same surface bound covalent anchor. Tsukruk and others extensively studied nanostructures generated with Y-shaped block copolymers.[29,40,59,65–67] The two branches of the Y-blocks are incompatible, so topography and morphology can again be controlled by polymer-solvent interactions.

Block copolymer brushes have also been immobilized on nanoparticle surfaces to generate tunable surface coatings.[68] Y-shaped copolymer blocks have been used to help form stable suspensions at aqueous/organic interfaces for nanodiamond[65] and gold nanoparticles.[67] Minko and coworkers polymerized poly(styrene)-*b*-poly(4-vinylpyridine) to generate controllable, hierarchical aggregates of block copolymer nanoparticles in solution, which can also form superhydrophobic surfaces when heated.[69] The surface free energy of the polymer nanoparticles can be tuned by selectively solvating PS or P4VP with toluene and acidic water, respectively. Grafted block copolymers can also template the formation of gold nanoparticles as demonstrated by Chen *et al.* in polymerization of 2-dimethylaminoethyl methacrylate (DMAEMA) *via* ATRP onto polymer micelles of polystyrene-*b*-polyethylene glycol. The grafted block intercalates into the nanoparticle coronal chains. By controlling micelle morphology at different pH values, the PDMAEMA can direct the formation of different sized gold nanoparticles in the micelle corona.[14]

The nanostructuring of block copolymer brush assembly is not limited to solvent switchability. Polymer brushes of poly(2-succinyloxyethyl methacrylate-*b*-N-isopropylacrylamide) (PSEMA-*b*-PNIPAM) show rearrangement behaviour in response to temperature and pH. The thermoresponsive PNIPAM block collapses above its lower critical solution temperature (LCST), while the PSEMA swells once it becomes deprotonated at higher pH. Using force–distance measurements on AFM, rearrangement of the blocks is confirmed for a combination of different temperatures and pH levels relative to homopolymer brushes, showing dual control over polymer brush morphology.[70] Ionic strength has also been used to induce nanoscale block copolymer morphology changes. Brash and coworkers studied polymers containing two hydrophilic blocks, poly(oligoethylene glycol methacrylate-*block*-trimethylammonium 2-methacryloxyoxyl ethyl chloride) (poly(OEGAMA-*b*-METAC)), where phase separation of the collapsed polymer occurred in increasing salt concentrations. They found the nanodomains could be as small as 10 nm, and tunable structures such as spheres, worms, and lines could be obtained.[71] Furthermore, this work demonstrated nanoscale templating of proteins by the selective adsorption of fibrinogen on the PMETAC domains which replicated the patterning of the phase separated polymer brush, without compromising the activity of the fibronectin.[71]

Block copolymer brushes have also been used to manipulate the migration of nanoparticles across a surface. Santer and Rühe described the motion of silica nanoparticles across poly(methyl methacrylate-*b*-glycidyl methacrylate) and poly(benzyl n-methacrylate-*b*-styrene) surfaces by vapor-induced microphase separation. The surface will reversibly form craters and hills, which can be used to transfer the nanoparticle across domains, as depicted in Scheme 1. By controlling the degree of polymerization of the first block, specific nanostructures can be formed such as ripples, worms and spheres.[26]

Recent work by Cheng and Cao describe the design of a temperature controlled nanofluidic gate using the triblock copolymer brush poly(styrene-*b*-acrylic acid-*b*-styrene).[72] A microchannel functionalized with the block copolymer brushes is heated to extend the chains and prevent the flow of nanoparticles through the system, while cooling results in chain collapse, allowing flow to resume.[72]

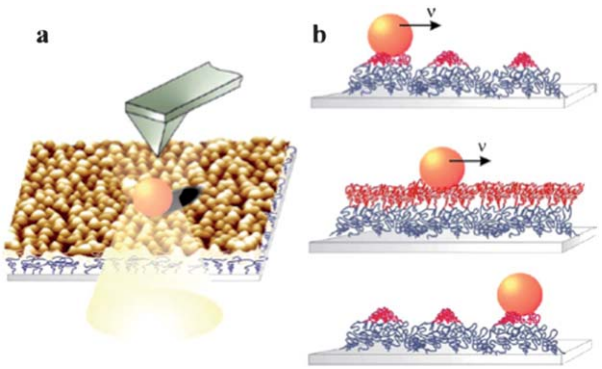

Scheme 1 (a) Scheme of a polymer brush carrying a cargo. (b) During topography switching accompanied by changes in the interfacial energy, the 'arms' of the brush grasp the nano cargo and move it along a surface.[26]

Gradient polymer brushes

Methods for forming gradients on surfaces have received much attention in recent years because gradients allow one to probe the effects of surface composition on a variety of interfacial phenomena. In polymer brush gradients, parameters such as grafting density (σ), molecular weight (MW), or composition are varied laterally on the surface. Such gradients are critical to improving the understanding physics of polymer brush systems, since one or more parameters can be varied on a single sample. Other applications include modification of microfluidic channels and studies of cell motility.

Self-assembled monolayers (SAMs) are an important factor in creating polymer brushes with a gradient in grafting density. A variety of techniques exist in the literature to vary the structure and composition of SAMs across a substrate including the formation of gradients by a vapor front,[73,74] cross-diffusion through a matrix,[75] electrochemical potential,[76] linear-motion drive,[77] and microcontact printing.[78] The examples listed above are early examples of monolayer gradients on the millimetre- to micrometre-scale.

To create SAM gradients on the nanometre scale is much more challenging and typically involves the use of hard lithography techniques. Ross *et al.* produced patterns in SAMs on gold by selectively removing alkanethiolates with a scanning tunneling microscope (STM).[79] This procedure involved coating a gold substrate with a SAM of $HS(CH_2)_{17}CH_3$, which functions as an ultrathin resist, which can then be etched by the STM tip. The treatment results in window like features that penetrate the organic monolayer. Patterns can be generated by STM that can ultimately form an initiator density gradient. STM-based lithography was taken further by Fuierer *et al.* by replacing the removed thiols with a ferrocenyl-based thiol.[80] In this report, varying a few STM parameters can produce complex gradient mesostructures. A direct-write "dip-pen" nanolithography technique has been developed by Piner *et al.* to deliver collections of molecules in a positive printing mode.[81] In this report, an atomic force microscope tip is used to "write" alkanethiols with a 30-nanometre line-width resolution on a gold thin film. Molecules are delivered from the AFM tip to the gold thin film *via* capillary transport. Others have used an alkane thiol gradient of any form and size down to several tens of nanometres, which can be "prewritten" by using an electron beam to irradiate a SAM followed by a subsequent exchange reaction of another alkanethiol.[82] This approach is more versatile, as one can choose among a broad range of molecular substituents.

The above techniques are very useful for forming gradients of initiators on surfaces that can ultimately be used to form polymer brushes with different grafting densities. Wu *et al.*[83,84] created a gradient in grafting density by covering the substrate with a gradient of initiator species utilizing the technique developed earlier by Chaudhury and Whitesides.[73] Polymerization of acrylamide from the surface-bound gradient of initiating sites was accomplished using ATRP. The thickness of the polymer is observed to be independent of the grafting density at low grafting densities. A crossover to the brush regime was observed to occur at a surface grafting density of 0.065 chains/nm^2 and thickness becomes largely dependent on grafting density. Poly(*tert*-butyl acrylate) (PtBA) brushes were also polymerized from an initiator gradient followed by conversion to poly(acrylic acid) (PAA), and the resulting wet thickness of the film was analyzed at varying pH values and ionic strength.[20] The approach to forming the initiator gradient was unique, where deposition of a gradient of inactive silane was done first, followed by subsequent backfilling with an ATRP initiator. In the resulting PAA brushes, it was observed that at low grafting densities, the polymer brush wet thickness remained constant, however, at $\sigma = 0.08$ chains/nm^2, the thickness follows the scaling law where $H \approx \sigma^{1/3}$. The thickness also becomes dependent on the ionic strength of the solvent. Another report utilized a "grafting to" approach, where Ionov *et al.* used a temperature gradient to control the kinetics of polymer grafting to form a gradient in grafting density.[9] No pre-existing gradient in initiator density was required. Grafting density gradients of PNIPAM brushes were synthesized by Wang *et al.* utilizing an electrochemical gradient to selectively desorb hexadecanethiol from a gold substrate followed by backfilling with the ATRP initiator.[19] Steenackers *et al.* successfully created polymer brushes of PMMA by self-initiated photografting and photopolymerization (SIPGP) from cross-linked biphenyl thiol SAMs.[85] Cross-linking the biphenyl thiol SAM was accomplished with a focused electron beam, where the beam energy was increased linearly over different areas of the substrate. In the presence of UV light, the non-crosslinked biphenyl thiols desorb and SIPGP occurs selectively on the cross-linked biphenyl thiols. Defined micro-and nano-structured polymer brush patterns were prepared with features as small as 50 nm.

In polymer brush systems, not only can one create a gradient based on grafting density, but also molecular weight. A gradient in polymer brush molecular weight was developed by Tomlinson *et al.* by covering a silicon wafer with chemisorbed ATRP initiator and placing it vertically into a solution of monomer (Fig. 1).[86] During the reaction, a micropump removes the solution from the chamber causing a steady decrease in the solution height. Varying the solution removal rate can control the profile of the polymer brush length gradient on the substrate. A dry PMMA brush height change from 0 to 22 nm was obtained in an almost linear fashion at a lateral distance of 25 mm across the substrate. Harris *et al.* presented a novel method based on an earlier report by Higashi *et al.*[87] for using photoiniferter-mediated photopolymerization techniques to create molecular weight

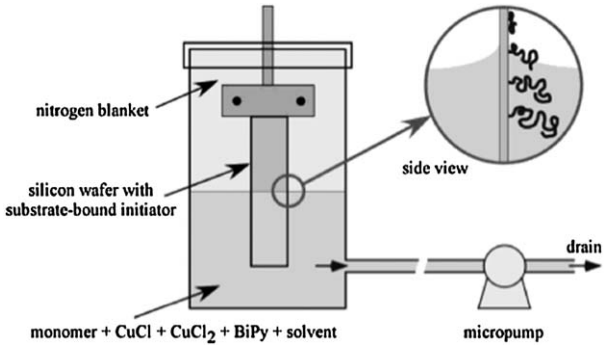

Fig. 1 Schematic of the apparatus for creating surface- grafted polymer assemblies with a gradient in molecular weight.[86]

gradients of PMMA and poly(methylacrylic acid) (PMAA).[88] Using a movable photomask permits creation of a UV exposure time gradient along the substrate. The control over chain density by this method has been taken further by functionalizing with an arginine-glycine-aspartic acid sequence to control cell adhesion across a substrate. Tomlinson *et al.* also successfully created a composition gradient of PHEMA-*block*-PMMA *via* ATRP.[18] A gradient in the first poly(hydroxylethyl methacrylate) (PHEMA) block is simply made by gradually removing the solution of monomer as demonstrated by Wu *et al.* Because a bromine atom remains at the chain terminus after ATRP polymerization, a block copolymer brush can be made *via* reinitiation. The substrate is subsequently placed in a solution of methyl methacrylate (MMA) without gradual removal of monomer to create a gradient in PHEMA, but not in MMA. Another option is to create a gradient in both PHEMA and MMA by also using the solution draining technique during polymerization of the second block. In another report by Xu *et al.* ATRP can be carried out inside microchannels to produce flat gradient and patterned surfaces.[89] Poly(dimethylamino-ethyl methacrylate) (PDMAEMA)-*b*-poly(butyl methacrylate) (PBMA) brush gradients consisting of a uniform PBMA bottom block and a molecular weight gradient PDMAEMA top block were also synthesized by gradually filling the polymerization chamber containing the PBMA brush coated substrate with the second ATRP solution.[90]

The synthesis of mixed polymer brushes with a unidirectional gradient in composition has also been described.[91] Treatment of this mixed brush composition with selective solvents revealed unique switching behaviour, where only one of the polymer brushes is well solvated and in its extended conformation as was described earlier. A combinatorial approach has also been used to study the effect of relative grafting density.[92] Grafting density gradients of two chemically different polymer brushes (PMMA/PS) propagating in opposite directions were synthesized from a binary mixed initiator layer by combining ATRP and NMRP in two steps. After treatment of the brush with glacial acetic acid, a selective solvent for PMMA, nanopatterns composed of relatively ordered nanoscale domains were observed in the region where the ratio of PS to PMMA grafting density was in the range from 0.67 to 2.17 chains/nm^2 and the overall grafting density was 0.85 chains/nm^2. Tomlinson *et al.* utilized such gradient copolymer structures to map out the influence of block length on surface morphologies of PHEMA-*b*-PMMA in response to selectively collapsing the top PMMA block of the copolymer.[93] Since there is no gradient in grafting density, the dry thickness of each block is directly proportional to its MW. Wang *et al.* utilized an electrochemical-gradient to generate mixed polymer-brush gradients of poly(*N*-isopropylacrylamide) (PNIPAM) and PHEMA.[94] Starting from a spatially uniform layer of initiator, a PNIPAM brush layer was grown. Then an in-plane electrochemical gradient was applied, which removed the PNIPAM brush preferentially at more negative potentials. The remaining active initiator sites were quenched followed by backfilling of the exposed gold regions with thiol initiator to generate an initiator density gradient from which a PHEMA was polymerized to achieve counter-propagating grafting density gradients of PNIPAM and PHEMA.

Orthogonal polymer brush gradients are also possible, in which two parameters (grafting density and molecular weight) are varied independently in orthogonal directions. Each point on an orthogonal gradient substrate is a unique combination of two surface properties, and Genzer and coworkers have used surface-initiated radical polymerization techniques to create such systems. Fabrication of surface grafted orthogonal gradients can be achieved in two steps: (1) the formation of a concentration gradient of initiator molecules followed by (2) the creation of a molecular weight gradient perpendicular to the initiator density gradient. It is also possible to hold constant one parameter while varying the other. This has been demonstrated by Bhat *et al.*,[95] where orthogonal gradients were used as functional combinatorial templates to direct the assembly of nanoparticles. Immersion of the gradient substrate of poly(dimethylamino-ethyl methacrylate) (PDMAEMA) in a pH 6.5 solution of nanoparticles allowed an electrostatic interaction between the DMAEMA groups in the brush and the citrate groups absorbed on the surface of the nanoparticles.

The formation of polymer brush gradients has been applied to manipulate nanoparticles across surfaces. In order to move nanosized objects, the surrounding polymer brush environment must be on the same order of magnitude as the object. Gradients are needed, therefore, where the slope changes drastically across lengths as low as 100 nm. A recent report by Schuh *et al.* has demonstrated such a polymer brush gradient by a unique combination of interference lithography and surface-initiated photopolymerization.[96] A UV-interference pattern is used to partially destroy a SAM of photoinitiator, followed by SIP of the initiators that remain intact. To generate the UV-interference pattern in the SAM, a parallel beam of light was partly reflected from a mirror positioned perpendicular to the surface. This arrangement leads to an interference pattern with strong fluctuations in light intensity that illuminates the surface. The UV light decomposes the initiator only in illuminated areas. By varying the angle of the interfering light beams in the patterning step, polymer brushes with different sized nanostructures could be prepared. Additionally, superimposing two UV light patterns generates more complex patterns. A mixed polymer brush with a gradient in composition was also accomplished in this report by simply performing a short (10 min) polymerization of N,N-dimethylacrylamide (DMAA) from an unstructured SAM. The remaining unreacted initiators were then partially deactivated using the interference process, followed by a second

polymerization of MMA from the surviving initiators to create a composition gradient where DMAA has a constant graft density, but the grafting density of MMA fluctuates at the nanometre scale.

Stimuli-responsive polymer brushes

Stimuli-responsive polymers are materials that respond in a controlled and predictable manner to external triggers, such as changes in temperature,[97,98] solvent,[99] pH,[100] applied mechanical force,[101] light,[102,103] and exposure to electrical and magnetic fields.[104] When grafted on a surface in high density, responsive polymers can be used for a wide variety of applications such as surface wettability, micro- and nano-fluidics, electronics, mechanical actuation, chemical sensing, biocompatibility, and controlled drug release. The generation of nanostructures typically is used to amplify these responses. The following section focuses on a review of recent advancements made in the field of stimuli-responsive homopolymer and copolymer brushes.

For applications related to the changing of wettability, stimuli-responsive polymer brushes are an excellent material to consider as they frequently undergo large changes in surface free energy when switching from one conformation to another upon exposure to an external stimulus. Temperature and light are two of the most widely used stimuli to induce changes in wettability. A well-known temperature-responsive polymer, PNIPAM, which has a LCST of 32 °C and will undergo a phase transition due to changes in solvent quality and temperature, is widely studied for its ability to switch surface wettability.[97,105] At temperatures below the LCST, the predominantly intermolecular hydrogen bonding between the PNIPAM chains and water molecules contributes to the hydrophilicity of the film. At temperatures above the LCST, however, this H-bonding is disrupted, resulting in a compact and collapsed conformation of the PNIPAM chains. This makes it difficult for the hydrophilic C=O and N–H groups to interact with the water molecules leading to a hydrophobic PNIPAM film. For example, PNIPAM was polymerized on both flat and rough silicon substrates using ATRP to show changes in contact angle between 63.5° to about 150° for rough surfaces formed by microlithography, when the temperature is increased from 25 °C to 40 °C.[97] Others have prepared polymer grafts of PNIPAM by ATRP on nano-textured substrates in which changes in macroscopic wettability are likely due to changes in the nanoscopic topography of the surface associated with expansion and contraction of the grafted polymer layer, as well as changes in the hydrophobicity of the polymer as it passes through its transition temperature.[106] Large changes in contact angle were observed as the pore size of the substrates was increased, with a change from about 13° to about 112° with a large pore size. PNIPAM has also been copolymerized on various substrates to enhance wettability changes.[107–111] Other thermo-responsive surfaces have been obtained by growing brushes of poly(2-(2-methoxyethoxy)ethyl methacrylate-*co*-oligo (ethylene glycol)) copolymers,[112] poly-*N*-[(2,2-dimethyl-1,3-dioxolane)methyl]acrylamide (PDMDOMA), and poly-zwitterionic hydrogels[113,114] which also undergo temperature dependent changes in surface wettability.

Light-induced conformational changes in a polymer brush can also affect the surface wettability. Locklin and coworkers used spiropyran-(SP) containing polymers and copolymers to show large changes in wettability due to the large change in dipole moment between the two photo-isomeric states of spiropyran, the ring-closed, nonpolar SP and the ring-opened, zwitterionic merocyanine (MC).[102,103] Upon ring-opening, divalent metal cations, such as Co^{2+} and Fe^{2+}, can complex to the phenolate anion of MC and stabilize the ring-open form. This can provide contact angle changes of up to 70°, depending on the metal cation used for complexation.

Polyelectrolyte brushes show large conformational changes in response to alternating ionic strength and pH, which can be used to alter surface wettability. The most common examples include homopolymer, mixed, and block copolymer brushes containing poly(acrylic acid) (PAA).[29,50,56,115–120] Other ionic liquid polymer brushes have also been used to tune wettability by exchanging their counterions.[121,122] A three stage switching of wettability has been observed using phosphate-containing polymer brushes, which undergo conformational changes at different pH, due to different chemical states from the association-dissociation equilibrium.[123] The Huck group has synthesized cationic poly(2-(methacryloyloxy)ethyltrimethylammonium chloride) brushes and studied the changes of its physical and chemical properties after brush collapse driven by ion-pairing interactions in the presence of ClO_4^- anions. With this system, ion-pairing interactions can be used to reversibly switch surface characteristics from hydrophilic to hydrophobic.[124] They have also exploited the use of electrochemical potentials to change the redox state inside the polyelectrolyte brushes, and as a consequence, the wettability of the brushes.[104]

Mechanical actuation is another application for which stimuli-responsive polymers have found utility. The actuation of cantilevers based on solvent changes, pH and ionic strength changes have all been observed.[123,125–127] Zhou *et al.* have also applied alternating voltage bias to induce cantilever deflections using a polyelectrolyte brush.[128] In all of these cases an external stimulus is applied to induce a mechanical change, but it is also possible to have polymer brushes that change chemically in response to a mechanical stimulus in an attempt to mimic the phenomenon in biology known as mechanotransduction.[101] A mechanical force is used to trigger a change in ionic strength inside the brush.

Polymer brush–nanoparticle assemblies

Nanostructured interfaces using polymer brushes have also been studied on nanoparticles themselves, leading to great opportunities for a range of applications including sensors, medical diagnostics, information storage, surface-enhanced Raman scattering, and phenomena involving local surface plasmon resonance. Surface-initiated polymerization techniques have been used to graft polymers from various nanoparticle surfaces, including silica,[129–136] gold,[137–142] clay[143,144] and several studies on the phase behaviour of well-defined mixed polymer brushes on silica nanoparticles have been reported.[145–149]

Additionally, stimuli-responsive polymers have been polymerized from nanoparticles in an effort to enhance the properties of nanoparticle–polymer brush hybrid nanostructures. Polymer brushes incorporating spiropyran have been a popular choice to functionalize nanoparticles as these materials display unique

properties upon exposure to light.[145] Hybrid silica nanoparticles grafted with poly(NIPAM-*co*-4-(2-acryloyloxy-ethylamino)-7-nitro-2,1,3-benzoxadiazole (NBDAE))-*b*-poly(NIPAM-*co*-spiropyran methacrylate (SPMA)) chains were fabricated by sequential SI-ATRP. At the surface of the silica core, this block copolymer brush collapses at temperatures above 37 °C due to the LCST of the NIPAM layer. Upon UV irradiation, the SPMA moieties in the outer layer of the polymer brush ring-open to give the fluorescent merocyanine form, leading to the occurrence of the fluorescence resonance energy transfer (FRET) process between the FRET donor, NBDAE and the photoswitchable acceptor, SPMA. Upon visible light irradiation, MC reverts back to the non-fluorescent SP, turning off the FRET process. This approach gives a system where hybrid silica nanoparticles are capable of emitting multi-color fluorescence, which can be easily tuned by UV irradiation, visible light, and temperature.

Thermosensitive polymer brushes, like PNIPAM, are commonly grown from gold nanoparticles.[147,148] Ion and pH responsive nanoparticle-polymer brush hybrids have also been fabricated.[149] Poly(2-(diethylamino)ethyl methacrylate) (PDEAEMA) brushes have also been grown from various nanoparticles for pH-responsive controlled release of encapsulated molecules[150] and for synthetic nanopores that can mimic the gating function of biological nanopores.[149]

Recent research has also been directed toward the positioning of nanoparticles in complex two- and three-dimensional structures using polymer chains tethered by one end to an underlying substrate in brush conformation.[151,152] Hybrid nanoassemblies were fabricated to demonstrate that localized surface plasmon resonance (LSPR) can be used detect the reversible stretching and shrinking motion of the PNIPAM chains in water upon changes in temperature.[153] The local effective refractive index of the film in water is greater at temperatures above the LCST, thereby shifting the LSPR peak to a longer wavelength at 40 °C. Tokareva *et al.* fabricated a nanosensor based on the real-time determination of swelling and shrinking of pH responsive poly(2-vinylpyridine) incorporated with gold nanoparticles to enhance transmission surface plasmon resonance spectroscopy.[154] Nanosensors specific for the presence of organic solvents in surrounding media have been developed based on the solvent induced swelling and deswelling of polymer brushes coupled with optical changes in localized surface plasmon resonance of gold nanoparticles.[155] Poly(NIPAM)–gold nanoparticle assemblies have also been designed towards applications for surface enhanced Raman spectroscopy[156] and temperature nanosensors.[157] Diamanti *et al.* created a template for post functionalization of polymer brushes which enables a wide variety of polymer brush–gold nanoparticle hybrids.[158] This provides a single, conceptual platform that enables the tuning of nanoparticle–surface interactions, which in turn will afford a wide range of technological opportunities.

Electron beam lithography

Nano-patterned polymer brush interfaces can be fabricated using advanced lithographic techniques in a top-down approach to tailor surface structure and morphology. The patterning required in nanofabrication is usually carried out with the photolithographic method employing deep UV radiation, where the wavelength of the light source is a large limitation on feature size. Efforts are now focused on using electron beam lithography techniques, where the wavelength is less than a tenth of a nanometre. One exception is the use of a nonlinear laser processing technique that is capable of generating sub-100 nm features.[159]

Maeng *et al.* utilized ATRP to fabricate patterned polymer brushes from a patterned initiator layer.[160] The patterned initiator layer was obtained through the use of a low energy electron beam and mask, which cleaved the halide group necessary for ATRP initiation. To minimize scattering, the employed electron energy was kept at 1.0 keV. Use of a higher energy beam of 30 keV resulted in very little polymer brush formation due to destruction of initiating sites *via* scattering effects. Brush patterns with a 6.5 μm line width were obtained. The patterning technique has also been used to create rectangular patterns of PS-*b*-PMMA and PS brushes.[160] To pattern the PS layer, a 3.0 keV electron energy was used to degrade the bromide sites at the end of the PS chains. A PMMA layer was then polymerized from the patterned PS layer to generate a patterned PS-*b*-PMMA with line widths of 6.0 um.

Another report by Schmelmer *et al.* utilized electron beam irradiation with nitro-1,1′biphenyl-4-thiol monolayers to selectively reduce the nitro functionality and crosslink the biphenyl layer.[161] The terminal amino groups are then diazotized and treated with methylmalonodinitrile to give a patterned monolayer of 4′-azomethylmalonodinitrile-1,1′biphenyl-4-thiol, which is suitable for use as initiators for radical polymerization. Following exposure to a solution of styrene at 80 °C, the polymerization was initiated *via* thermal decomposition of the initiator layer. Amplified patterns with AFM height profiles show polymer brush line widths as small as 70 nm.

Micro- and nano-patterns of pNIPAM brushes have also been created by He *et al.*[162] Electron beam patterning through a mask allowed the generation of features sizes down to 70 nm in width by crosslinking a 4′-nitro-1,1′-biphenyl-4-thiol monolayer, which also reduced the nitro to an amine by the electron beam. The resulting patterned amine was treated with bromoisobutyryl bromide to create a patterned surface bound ATRP initiator. Exposure of this initiator to NIPAM results in a brush layer. Another report by Schmelmer *et al.* presented the use of a high focused electron beam instead of a mask to create patterns.[163] This allowed for sub-50-nm polymer brush features to be grown from patterned, cross-linked initiator sites *via* surface-initiated photopolymerization of styrene. Polymer brushes of defined thickness have also been created using methyl methacrylate and *tert*-butyl methacrylate from cross-linked benzyl-, phenyl-, and hydroxyl-functionalized SAMs.[85] Since only an electron beam sensitive SAM is needed, this approach is more versatile to many complex polymer structures and architectures.

Domain sizes of polymer brushes generated by photolithographic patterns of initiator followed by SIP are limited at the lower end due to lateral spreading of polymer chains at the domain boundaries, which leads to poorly defined features. For this reason, electron beam lithography to form nanostructured polymer brushes by post-polymerization patterning is a viable alternative, and has been initially investigated by Ober and coworkers. To entirely bypass complex lithographic schemes, Rastogi *et al.* used an electron beam to directly pattern polymer brushes of PMMA, PHEMA, poly(isobutyl methacrylate)

(PIBMA), poly(neopentyl methacrylate) (PNPMA), and poly (2,2,2-trifluoroethyl methacrylate) (PTFEMA) grown *via* ATRP from silicon substrates.[164] Patterns with features as small as 50 nm were obtained. The order in increasing sensitivity toward electron beam irradiation among the different brushes was found to be PMMA < PIBMA < PHEMA ≈ PNPMA < PTFEMA. This finding demonstrates that one can tailor-make polymer brushes to be highly sensitive toward electron beam irradiation by chemical modification at the β-position to the carbonyl group. Super critical carbon dioxide ($scCO_2$) has been used following the electron beam patterning step to develop the patterned brushes *via* removal of the degraded polymer.[165] Typically, THF is used for this step, but $scCO_2$ has several advantages. Along with economic viability, the high diffusivity and low viscosity of $scCO_2$ allows for its efficient removal *via* depressurization. A large variation in solubility can be achieved with small changes in operating conditions. Paik *et al.* took the direct electron beam patterning of polymer brushes even further by creating a patterned block copolymer with a negative tone upper layer (PS) and a positive tone under layer (PMMA or PHEMA) to create channels (Fig. 2).[165]

Other hard lithographic techniques

While electron beam lithography has been more prominent in formation of polymer brush nanostructures with small features, other lithography techniques have also been studied to form nanoscale polymer brush surfaces. Atomic force microscopy, dip pen lithography, nanoshaving, and scratch card lithography have all used scanning probe tips for polymer brush nanopatterning.[15,166–170] The Kanoufi group used a scanning electrochemical microscope to perform rapid electrochemical reductions of ATRP monolayers in micropatterned domains. In varying the reducing strength of the probe, initiator density was systematically varied for SIP.[170] AFM cantilevers with an applied electric field have also been used to selectively oxidize silicon to template the fabrication of nanopattern polymer brushes with lateral dimensions as small as 300 nm.[169] Kaholek *et al.* presented a new and simple strategy to fabricate stimuli-responsive, surface-confined PNIPAM brush nanopatterns.[168,171] This was accomplished by combining SIP and "nanoshaving," which gave patterns of 500 nm × 10 μm. Nanoshaving uses an AFM tip to selectively remove a thiol resist under high tip forces (~50 nN) and high scan rates (~20 μm s^{-1}). A gold substrate coated with octanethiol is removed from the surface, and the freshly exposed portions of the substrate are exposed to an ATRP thiol initiator. A reversible, stimuli-responsive conformational height change of these nanopatterned polymer brushes was demonstrated. Kaholek and coworkers also utilized a "top-down/bottom-up" strategy to fabricate nano- and micro-patterned polymer brush arrays composed of weak polyelectrolyte copolymers of poly(*N*-isopropylacrylamide-*co*-methacrylic acid).[172] Electron beam patterning of a PMMA-coated substrate followed by gold deposition allowed the formation of a gold patterned silicon substrate after removal of the resist. A thiol-based azoinitiator was self-assembled on the gold patterns and amplified by photopolymerization to generate micro- and nano-patterned poly (NIPAM-*co*-MAA) with lateral dimensions ranging from 550 nm to 3.4 μm. This brush is sensitive to both pH and ionic strength, and it was shown that in the presence of water at pH 9.0 the dry polymer swells by more than one order of magnitude (9 nm to 112 nm in height). This is a result of the carboxylic acid groups in the MAA comonomer being deprotonated, which leads to chain stretching. In the presence of water at pH 4.0, the brush collapses (112 nm to 9 nm) and this process is reversible. Adding salt to the stretched brush in basic media causes the brush to collapse, due to screening of the charged carboxylic acid groups. In this report, use of gold patterns on silicon has a few advantages, including well-defined features that can be created over large areas, the ability to fabricate mixed polymer brushes utilizing silane- and thiol-based initiators, and a wide variety of chemistries using different monomers.[172] Ahn *et al.* utilized the same technique to create micro-patterned lines of PNIPAM (1.8 μm wide, 300 nm high) with a dot nano-pattern (600 nm wide, 170 nm high) contained within the lines.[173]

Morsch *et al.* described "scratch card" lithography as a method to create nanoscale polymer brush surfaces.[174] Scratch card lithography describes the pulsed plasma chemical deposition of an ATRP initiator layer, masked by a poly(vinylbenzyl chloride) layer, which is selectively removed by the scratching of the secondary layer with a scanning probe tip 100 nm wide.[174] The underlying initiator layer is exposed by scanning probe lithography for patterned surface initiation, while preserving the unexposed sites below for subsequent polymerizations using different monomers. They observed reversible domain size changes of the nanoscale polymer brushes based on the solvent-selective masking of functional surfaces.

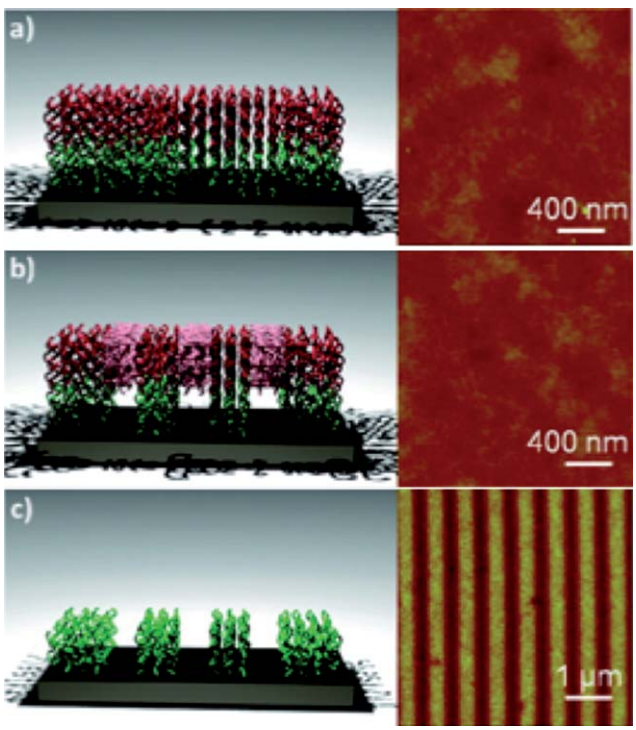

Fig. 2 An illustration representing the nanochannel fabrication process with corresponding AFM images. The diblock brush (a) undergoes electron beam exposure and development (b) followed by etching of the PS layer using oxygen plasma.[165]

Mirkin and coworkers took a different approach with dip pen lithography, where they deposited initiator and monomer in a two-step approach to patterned polymer brushes synthesized by ring opening metathesis polymerization (ROMP).[15] By controlling print time of monomers, they demonstrated control over the degree of polymerization on features as small as 100 nm in diameter.[15]

Soft lithography

To incorporate nanostructured polymer brush surfaces into larger scale patterning, simplified lithography techniques are required to replicate a patterned surface with high fidelity. While e-beam and other techniques are useful for generating nanoscale features, soft lithography, involving the patterning of surfaces through mild chemical or physical deposition is an alternative to templating nanostructured polymer brushes. Soft lithographic patterning of polymer brushes consists of three main methods: (1) microcontact printing of an initiator layer followed by polymerization, (2) patterning of a small molecule on top of an existing polymer brush, or (3) patterning of an inert polymer, for backfilled patterned polymerization, using techniques such as capillary force lithography.

Microcontact printing (μCP) is a chemical process where a stamp, formed usually out of PDMS, is coated with an organic solution and printed onto a surface. Microcontact printing has been used extensively to form nanoscale patterns of polymer brushes on surfaces,[105,175–183] with emphasis on polymer brush architectures with thermally switchable domains,[105] aqueous block copolymers,[184] and microphase separated polymer "anemones."[185]

While the majority of microcontact printing has been focused on nanoscale patterning of initiator layers, some research has focused on post polymerization modification. The Zauscher group used hydrogen bond-mediated microcontact printing of ATRP initators on exisisting poly(acrylic acid) brushes for the patterned block/graft copolymerization of NIPAM.[186] Domain size of the grafted copolymer brush pattern could be systematically controlled using both contact time and applied pressure of the stamp during μCP of the initiator on the PAA brush surface.

Two adaptations on μCP were developed by the Vaia group to pattern poly(ethylene glycol) (PEG) on functionalized poly(2-hydroxyethyl methacrylate) brushes for the immobilization of citrate-capped gold nanoparticles.[187] The first is reactive microcontact printing, where a PDMS stamp inked with PEG-amine is printed on the polymer brush to immobilize micron-scale stripes of gold nanoparticles. The second, reactive microcapillary printing, uses capillary action to draw fluid into the channels of an elastomeric stamp on the surface, creating a micropattern of PEG-amine.[187]

Nanoimprint lithography in thin film PMMA was conducted by the Huck group to generate nanoscale wells for NIPAM polymer brushes as small as 35 nm in domain diameter, representing roughly 300 grafted polymer chains. They demonstrated the responsive polymer could be controlled by lateral size control of the domains, allowing for tunable topographies, even with such a small collective motion of polymer chains.[166]

Capillary force lithography has also been utilized by Luzinov and coworkers to mold thin polystyrene films with feature sizes as small as 100 nm by drawing polymer into elastomer channels by capillary force at temperatures above the polymer glass transition temperature (T_g).[188] The exposed surfaces are then backfilled to selectively initiate controlled radical polymerization. The molded polystyrene layers can be removed by dissolving them in a miscible solvent, which creates a binary surface for further functionalization. This has also been accomplished with solvent assisted-"grafting to" polymerization to immobilize nanoparticles.[189]

Inimer patterning of polymer brushes

Carter and coworkers have designed a novel approach for manipulating the size and chemistry of nanoscopic features using a tandem, top-down/bottom-up approach that combines contact molding and living free radical polymerization.[190] In this technique, a network photopolymer that contains an embedded inimer (contains both initiator and monomer) is molded into patterned features (Scheme 2). In a secondary reaction step, polymer brushes of defined chemistry and structure are grown from the exposed imbedded inimers on the surface of the patterned network, thus changing the surface chemistry of the features, as well as the size of the features. This process is a simple and powerful method for growing controlled polymer brushes with a variety of different feature sizes and functional groups using the same molded template.

The primary patterning technique used in this approach is a top-down contact-molding imprint lithography process, which involves the use of a patterned polymeric mold to template a spin-cast film of an inimer-containing photopolymer solution that is subsequently UV-polymerized while in contact with the transparent pattern mold. This method has been used to fabricate well-defined polymer brushes consisting of PS, PMMA, and PHEMA linear chains using both atom transfer radical

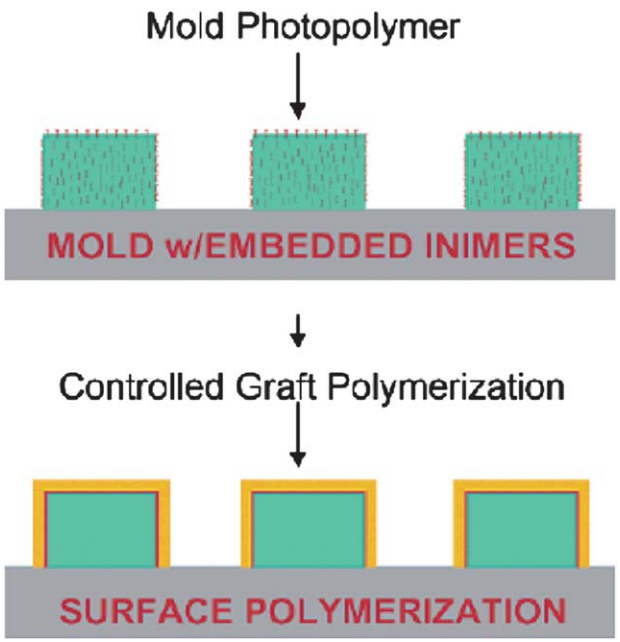

Scheme 2 Pictorial representation of surface tuning for nanoscopic pattern replication using embedded inimers.[190]

polymerization (ATRP) and nitroxide-mediated polymerization (NMP) initiated from the inimer-embedded surfaces.[190] Brushes with controlled thickness ranging from 10 to 143 nm were grown, and the feature sizes could be tuned from the original 100 nm down to 20 nm.

A thorough examination of each step in the process has been performed from substrate preparation to photopolymer attachment to polymer brush growth.[191] Several 3-methacryloxypropyl silane derivatives were evaluated as silane coupling reagents, where the 3-methacryloxypropyl functionality reacts in the photopolymerization of acrylate/methacrylate monomer films leading to high quality network films. An example of a polystyrene-d8 brush grown by NMP from these surfaces embedded with an alkoxyamine inimer was also demonstrated.

Carter and coworkers have also described a new procedure for surface grafting polyfluorene brushes by step-growth polymerization from initiator-embedded polymeric thin films and micron- and nanometre scale patterns using nanocontact molding.[191] More recently, nanocontact molding has been used to pattern biologically active materials by molding functional photopolymer resins to create controlled nanoscale patterns of a cross-linked photopolymer containing embedded alkoxyamine-based initiator groups.[192] Functionalized polymer brushes were grown from these patterned layers by NMP, where chain end functionalization was accomplished by nitroxide radical exchange during the polymerization process.

Multicomponent nanostructured polymer surfaces

The formation of multicomponent surfaces allows for the introduction of two or more types of polymer substrates in a well-defined, spatially-oriented area. This can assist in developing specialized nanostructures on surfaces and providing nanoscale surface with chemical specificity. While mixed and block polymer brushes have already been discussed in detail, multicomponent surfaces deal with patterned polymer brush domains that can be formed by two methods: (1) sequential polymerization of patterned surface initiators and/or (2) orthogonal surfaces by post-polymerization modification.

Sequential polymerization involves polymerization, followed by a surface activation step, such as etching of polymer or activation of a protected initiator species. Several papers have achieved binary functional polymer surfaces by post polymerization modifications to a polymer brush, followed by a second polymerization to backfill the bare regions.[193–195] Sequential polymer brush formation has also been achieved *via* microcontact printing by the Huck group.[196] This work went above and beyond the formation of binary functionalized surfaces, to generate up to eight quaternary functionalized surfaces by controlled polymerization (ATRP), passivation of the initiator endgroup, printing of a new initiator, and subsequential polymerization.[196] This technique demonstrates high fidelity polymer patterns that are amenable to several types of monomers with different chemical functionality. The complex surfaces showed no intercalation between brush layers, or the polymers synthesized from printed initiators on top of the underlying brush surfaces.

Multifunctional polymer brushes have also been used to form solid-supported and hollow shell nanostructures by modification of nanoparticle surfaces with orthogonally functionalized polymer brushes.[197] The development of polymeric mimics to biological systems is instrumental in applying controlled nanostructured surfaces to biomedical applications. Dual-click chemistry at alkyne and alkene surfaces with azide and thiolyne-functionalized polymers, respectively, can be utilized to form "hairy" nanoparticles and nanospheres with hydrophilic and hydrophobic portions, which may be useful for drug delivery or as red blood cell mimics.[197] Scanning electron and transmission electron micrographs of the nanospheres are shown in Fig. 3. Photolithography has been utilized by the Ober group to selectively polymerize polymer domains to template biological functionalization surrounded by protein-resistant poly(ethylene glycol).[198] Grafting from polymerization of poly[(2-methyacryloxyloxy)ethyl] trimethylammonium chloride (PMETA) in microdomains surrounded by polyethylene glycol were used for the directed growth of rat hippocampal neurons, which may find utility in the development of neural device coatings. The dual

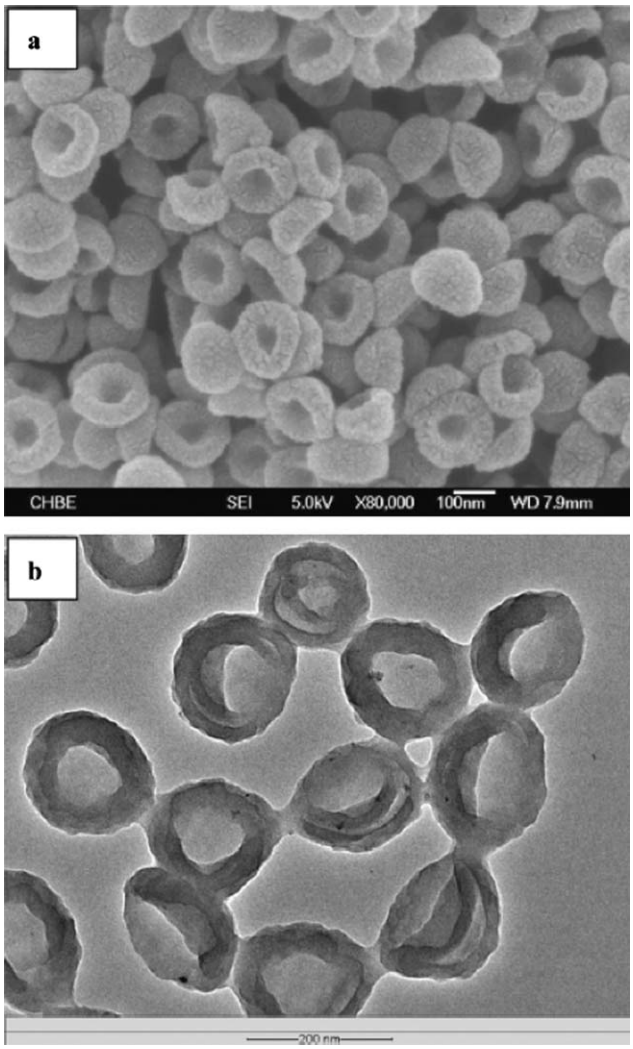

Fig. 3 (a) Scanning electron micrographs and (b) transmission electron micrographs hairy hollow nanospheres The scale bars for (a) and (b) are 100 and 200 nm, respectively.[197]

functionality of the cytophobic PEG and cytophilic PMETA allowed PMETA-facilitated neural growth.[198]

As specificity and functionality is demanded of polymeric surfaces on the nanoscale, the ability to customize and synthesize tunable surfaces becomes more and more critical. The second type of multifunctional surfaces stem from post polymerization activation of polymer brush pendant groups, mainly through photolithography. Specifically, a few groups have studied functional polymer brushes where pendant groups, such as thiolynes, alkynes, or n-hydroxysuccinimide esters, can be used to covalently bind a complimentary group in solution, attaching desired moieties along the polymer backbone. These polymer templates are advantageous in preventing the exhaustive optimization required when polymerizing a new monomer system and allow for rapid development of functionalized polymer brushes by photolithographic activation. Specifically, the Patton group used photopolymerized poly(propargyl methacrylate) to functionalize thiol terminated molecules in the radical-mediated thiol-yne click reaction, generated by ultraviolet light (254–470 nm).[199] Functionalizable polymer brush scaffolds based on n-hydroxysuccinimide esters have also been used to template multicomponent surfaces with spatially resolved functionality by modification with a photoactivated compound.[200] A cyclopropenone-amine was immobilized onto the polymer brush backbone, which can undergo decarbonylation to form a strained dibenzocyclooctyne when irradiated with UV light. This dibenzocyclooctyne then reacts rapidly with azides under ambient conditions without the use of metal catalysts.[200] The photoactivation of the polymer brush allows for selective activation and functionalization of different azides on separate microdomains without cross contamination.

Conjugated polymer nanostructures

In the past decade, a new interest in conjugated polymers (CPs) has emerged due to their potential in applications ranging from polymeric light emitting diodes (PLEDs) to photovoltaics. In photovoltaics, the ability to form nanoscale patterned donor and acceptor materials will allow for more efficient charge separation. While most reports of patterned conjugated polymers are accomplished through spin-coating or reacting a precursor polymer to a substrate followed by lithographic techniques, the creation of conjugated polymer brushes is still in the early stages of development.

Zotti *et al.* have performed the electrochemical anodic coupling of different pyrrole- and thiophene-based monomers to oligothiophene-based SAMs on indium tin oxide (ITO) and gold electrodes.[201] This resulted in grafting of conjugated polymer films from the electroactive monolayer. This technique is far superior to previous electrochemical techniques utilizing bare gold and platinum electrodes. This new method allows the formation of nanometre-sized layers of conjugated polymers with nominally normal orientation of the chain to the surface. Microcontact printing was used to pattern terthiophene-based monolayers onto gold and ITO electrodes, and the subsequent electropolymerization amplified the patterns, which was visible through AFM.

Beinhoff *et al.* developed a new procedure that utilized a step-growth Yamamoto-type Ni(0) mediated polymerization.[191] Nanocontact molding was used to prepare thin patterned crosslinked polyacrylate network films on silicon wafers that incorporated 4-bromstyrene in the networks. This 4-bromostyrene moiety presented a reactive sight for subsequent Yamamoto polymerization of 2,7-dibromo-,9,9-dihexylfluorene (PDHF). Brush growth was conducted from patterned features ranging from 100 μm to 100 nm in width and 50 nm in height. Another report by Moran *et al.* enhanced the rate and extent of grafting of PDHF by incorporating 2,7-dibromo-9-fluorenyl methacrylate (DBFM) as a new grafting agent in the crosslinked polymer resin.[202] Varying the concentration of DBFM controlled both overall graft formation and fluorescence. Microwave heating was used to obtain 30 nm of PDHF in as little as 30 min. Nanocontact molding was used to generate features ranging in size from 100 μm to 100 nm in width and 60 nm in height, followed by microwave-assisted grafting of PDHF. Grafting of PDHF resulted in fluorescent patterns that had an increase in height.

Surface-initiated Kumada catalyst-transfer polycondensation (SI-KCTP) has recently emerged as a viable strategy for forming conjugated polymer brushes from surfaces.[16,17] This new technique shows considerable promise and is still in its early stages of development. Khanduyeva *et al.* developed a unique nanostructured micelle by dissolving P4VP$_{75}$-*b*-poly(*p*-iodostyrene)$_{313}$ in hot toluene and allowing it to equilibrate at room temperature for at least for one week (Scheme 3).[203] These micelles were then spin-coated onto a silicon wafer and annealed at 150 °C. At this temperature, poly(*p*-iodostyrene) constituting the shell of the micelles does not melt and acts as nanoreactor in which molten P4VP chains will be grafted to the surface. Poly(3-hexylthiophene)) (P3HT) was then grafted from the poly(*p*-iodostyrene)

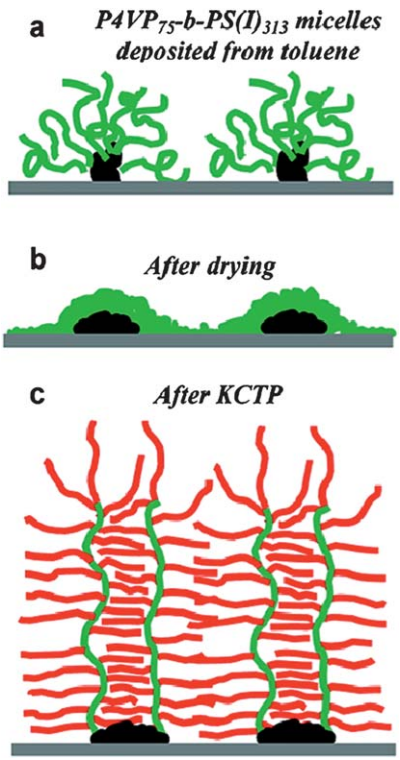

Scheme 3 Schematic representation of the formation of nanostructured P4VP-*b*-PS(I)-*g*-P3HT brushes.[203]

chains. Although the grafting of P3HT from the nanopatterned $P4VP_{75}$-*b*-poly(*p*-iodostyrene)$_{313}$ brush destroys the initial order, the particulate morphology in the resulting film was preserved. In another report utilizing SI-KCTP, Senkovskyy *et al.* immobilized the initiator on both nano- and micro-sized silica particles.[204] In the presence of monomer, P3HT was grafted from the particles.

Beryozkina *et al.* utilized a Suzuki-type polycondensation scheme to generate conjugated polymer brushes of poly(9,9-bis (2-ethylhexyl)fluorene) (PF2/6) up to 100 nm thick.[205] A colloidal-type lithography technique was used, where sub-micrometre hydrogel particles were arranged on silicon wafers by dip-coating. These particles were used as a mask during the treatment of octadecylsilane to deactivate the space between the particles. After removal of the particles, the exposed circular regions on the wafer were reacted with a silane-based initiator for Suzuki polycondensation. Subsequent polymerization of PF2/6 from the initiator sites generated microstructured conjugated polymer brushes where each round shaped disk was approximately 1 μm in diameter.

Conclusions

In this review, we have presented recent developments in the field of polymer brush chemistry that have been used to fabricate nanostructured materials. From these developments, two main themes arise in methods of nanostructured polymer brush fabrication: "bottom up" and "top down" nanostructures. Bottom up nanostructured brushes are described by stimuli responsive, mixed, block, inimer, and stimuli responsive polymer brushes, where the nanostructured surface is generated by properties unique to the polymer chemistry used, and can be induced by a macroscopic environment change, such as solvent, heat or light. Nano-scale patterned polymer brushes fabricated by a top down method, as demonstrated in the aforementioned examples using hard and soft lithography, and other photolithographic techniques used in nano gradients and multicomponent surface polymer brushes, are at the cutting edge of available technology in terms of spatial resolution and patterning.

Most of the examples of both top down and bottom up fabrication of polymer brush nanostructures are generated using commercially available monomers, such as styrene and methyl methacrylate. This has been necessary to understand the fundamental influences of polymer conformation, polymer brush chemistry and lithographic techniques on generating nanostructured surfaces. The next step in advancing nanostructured polymer brushes as a viable option in nanotechnology lies in combining top down and bottom up methods to pattern specialized, functional polymer brushes. For example, using e-beam lithography to pattern a conjugated polymer brush could generate nanostructured surfaces capable of better light-induced charge separation to develop more efficient photovoltaic devices. While recent literature has alluded to specialized polymer functionality in nanostructured surfaces,[199,200,206,207] new platforms and strategies are necessary to develop application specific chemistry on the nanoscale.

Furthermore, there will always be an inherent limit on the resolution to nanopattern surfaces from the top down. The "bottom up" approach is only be limited by the properties of the polymer chains attached to the surface. The union of stimuli-induced nano-architectures along with the incorporation of specialized homo- and copolymers is key into integrating polymer brush nanostructures into electronics, sensors and biomedical industries.

As the applications of nanotechnology become more interdisciplinary, polymer brushes provide a durable, controllable, and customizable interface between surfaces and the macroscopic environments they aim to influence. This review article has focused on recent advances of specialized polymer brushes on the nanoscale, but as polymer technology expands to include more advanced chemistries, architectures, and fabrication methods in solution, these macromolecules must eventually be evaluated on the nanoscale to compare different chemical and physical properties of polymer brushes relative to their bulk counterparts. Only when the ability to generate and control specialized polymer brushes on the nanoscale is demonstrated can we definitively say that nanostructured polymer brush interfaces have the ability to significantly impact larger, interdisciplinary fields.

The authors gratefully acknowledge financial support from the Donors of the American Chemical Society Petroleum Research Fund (Grant 48917-DNI7) and the National Science Foundation (ECCS 0901141, DMR 0953112, and CHE 1058631).

References

1 K. Ariga, *Phys. Chem. Chem. Phys.*, 2011, **13**, 4780–4781.
2 W. Senaratne, L. Andruzzi and C. K. Ober, *Biomacromolecules*, 2005, **6**, 2427–2448.
3 Y. Lei, W. Cai and G. Wilde, *Prog. Mater. Sci.*, 2007, **52**, 465–539.
4 Y. Wang, L. Hosta-Rigau, H. Lomas and F. Caruso, *Phys. Chem. Chem. Phys.*, 2011, **13**, 4782–4801.
5 W. J. Brittain and S. Minko, *J. Polym. Sci., Part A: Polym. Chem.*, 2007, **45**, 3505–3512.
6 S. T. Milner, *Science*, 1991, **251**, 905–914.
7 N. Ayres, *Polym. Chem.*, 2010, **1**, 769–777.
8 R. l. Barbey, L. Lavanant, D. Paripovic, N. Schüwer, C. Sugnaux, S. Tugulu and H.-A. Klok, *Chem. Rev.*, 2009, **109**, 5437–5527.
9 L. Ionov, B. Zdyrko, A. Sidorenko, S. Minko, V. Klep, I. Luzinov and M. Stamm, *Macromol. Rapid Commun.*, 2004, **25**, 360–365.
10 S. Minko, S. Patil, V. Datsyuk, F. Simon, K.-J. Eichhorn, M. Motornov, D. Usov, I. Tokarev and M. Stamm, *Langmuir*, 2002, **18**, 289–296.
11 F. Zhou and W. T. S. Huck, *Phys. Chem. Chem. Phys.*, 2006, **8**, 3815–3823.
12 V. N. Michailidou, B. Loppinet, O. Prucker, J. Rühe and G. Fytas, *Macromolecules*, 2005, **38**, 8960–8962.
13 S. Edmondson, V. L. Osborne and W. T. S. Huck, *Chem. Soc. Rev.*, 2004, **33**, 14–22.
14 K. Chen, D. Liang, J. Tian, L. Shi and H. Zhao, *J. Phys. Chem. B*, 2008, **112**, 12612–12617.
15 X. Liu, S. Guo and C. A. Mirkin, *Angew. Chem., Int. Ed.*, 2003, **42**, 4785–4789.
16 V. Senkovskyy, N. Khanduyeva, H. Komber, U. Oertel, M. Stamm, D. Kuckling and A. Kiriy, *J. Am. Chem. Soc.*, 2007, **129**, 6626–6632.
17 S. K. Sontag, N. Marshall and J. Locklin, *Chem. Commun.*, 2009, 3354–3356.
18 M. R. Tomlinson and J. Genzer, *Chem. Commun.*, 2003, 1350–1351.
19 X. Wang, H. Tu, P. V. Braun and P. W. Bohn, *Langmuir*, 2006, **22**, 817–823.
20 T. Wu, P. Gong, I. Szleifer, P. Vlček, V. r. Šubr and J. Genzer, *Macromolecules*, 2007, **40**, 8756–8764.
21 B. Zhao, *Langmuir*, 2004, **20**, 11748–11755.
22 A. Sidorenko, S. Minko, K. Schenk-Meuser, H. Duschner and M. Stamm, *Langmuir*, 1999, **15**, 8349–8355.
23 I. Luzinov, S. Minko and V. V. Tsukruk, *Prog. Polym. Sci.*, 2004, **29**, 635–698.

24 P. Uhlmann, L. Ionov, N. Houbenov, M. Nitschke, K. Grundke, M. Motornov, S. Minko and M. Stamm, *Prog. Org. Coat.*, 2006, **55**, 168–174.
25 I. Luzinov, S. Minko and V. V. Tsukruk, *Soft Matter*, 2008, **4**, 714–725.
26 S. Santer and J. Rühe, *Polymer*, 2004, **45**, 8279–8297.
27 J. Zhang, Y. Yang, C. Zhao and H. Zhao, *J. Polym. Sci., Part A: Polym. Chem.*, 2007, **45**, 5329–5338.
28 D. Julthongpiput, Y.-H. Lin, J. Teng, E. R. Zubarev and V. V. Tsukruk, *Langmuir*, 2003, **19**, 7832–7836.
29 D. Julthongpiput, Y.-H. Lin, J. Teng, E. R. Zubarev and V. V. Tsukruk, *J. Am. Chem. Soc.*, 2003, **125**, 15912–15921.
30 B. Zhao and T. He, *Macromolecules*, 2003, **36**, 8599–8602.
31 B. Zhao, R. T. Haasch and S. MacLaren, *J. Am. Chem. Soc.*, 2004, **126**, 6124–6134.
32 B. Zhao, R. T. Haasch and S. MacLaren, *Polymer*, 2004, **45**, 7979–7988.
33 J. Feng, R. T. Haasch and D. J. Dyer, *Macromolecules*, 2004, **37**, 9525–9537.
34 B. Zhao, D. Li, F. Hua and D. R. Green, *Macromolecules*, 2005, **38**, 9509–9517.
35 F. Hua, X. Jiang, D. Li and B. Zhao, *J. Polym. Sci., Part A: Polym. Chem.*, 2006, **44**, 2454–2467.
36 M. Lemieux, S. Minko, D. Usov, M. Stamm and V. V. Tsukruk, *Langmuir*, 2003, **19**, 6126–6134.
37 J. Draper, I. Luzinov, S. Minko, I. Tokarev and M. Stamm, *Langmuir*, 2004, **20**, 4064–4075.
38 L. Ionov, A. Sidorenko, K.-J. Eichhorn, M. Stamm, S. Minko and K. Hinrichs, *Langmuir*, 2005, **21**, 8711–8716.
39 K. Yu, Y. Cong, J. Fu, R. Xing, N. Zhao and Y. Han, *Surf. Sci.*, 2004, **572**, 490–496.
40 Y.-H. Lin, J. Teng, E. R. Zubarev, H. Shulha and V. V. Tsukruk, *Nano Lett.*, 2005, **5**, 491–495.
41 Y. Mikhaylova, L. Ionov, J. r. Rappich, M. Gensch, N. Esser, S. Minko, K.-J. Eichhorn, M. Stamm and K. Hinrichs, *Anal. Chem.*, 2007, **79**, 7676–7682.
42 S. Minko, D. Usov, E. Goreshnik and M. Stamm, *Macromol. Rapid Commun.*, 2001, **22**, 206–211.
43 M. Motornov, S. Minko, K.-J. Eichhorn, M. Nitschke, F. Simon and M. Stamm, *Langmuir*, 2003, **19**, 8077–8085.
44 S. Minko, M. Müller, D. Usov, A. Scholl, C. Froeck and M. Stamm, *Phys. Rev. Lett.*, 2002, **88**, 035502.
45 D. Usov, V. Gruzdev, M. Nitschke, M. Stamm, O. Hoy, I. Luzinov, I. Tokarev and S. Minko, *Macromolecules*, 2007, **40**, 8774–8783.
46 S. Santer, A. Kopyshev, H.-K. Yang and J. r. Rühe, *Macromolecules*, 2006, **39**, 3056–3064.
47 S. Minko, I. Luzinov, V. Luchnikov, M. Müller, S. Patil and M. Stamm, *Macromolecules*, 2003, **36**, 7268–7279.
48 M. C. LeMieux, D. Julthongpiput, K. N. Bergman, P. D. Cuong, H.-S. Ahn, Y.-H. Lin and V. V. Tsukruk, *Langmuir*, 2004, **20**, 10046–10054.
49 J. Wang and M. Müller, *J. Phys. Chem. B*, 2009, **113**, 11384–11402.
50 L. Ionov, N. Houbenov, A. Sidorenko, M. Stamm, I. Luzinov and S. Minko, *Langmuir*, 2004, **20**, 9916–9919.
51 L. Ionov, S. Minko, M. Stamm, J.-F. o. Gohy, R. Jérôme and A. Scholl, *J. Am. Chem. Soc.*, 2003, **125**, 8302–8306.
52 L. Ionov, N. Houbenov, A. Sidorenko, M. Stamm and S. Minko, *Adv. Funct. Mater.*, 2006, **16**, 1153–1160.
53 M. Motornov, R. Sheparovych, I. Tokarev, Y. Roiter and S. Minko, *Langmuir*, 2007, **23**, 13–19.
54 S. Santer, A. Kopyshev, J. r. Donges, J. r. Rühe, X. Jiang, B. Zhao and M. Müller, *Langmuir*, 2007, **23**, 279–285.
55 S. Santer, A. Kopyshev, J. r. Donges, H.-K. Yang and J. r. Rühe, *Langmuir*, 2006, **22**, 4660–4667.
56 N. Houbenov, S. Minko and M. Stamm, *Macromolecules*, 2006, **36**, 5897–5901.
57 M. Motornov, R. Sheparovych, E. Katz and S. Minko, *ACS Nano*, 2008, **2**, 41–52.
58 M. Lemieux, D. Usov, S. Minko, M. Stamm, H. Shulha and V. V. Tsukruk, *Macromolecules*, 2003, **36**, 7244–7255.
59 M. C. LeMieux, S. Peleshanko, K. D. Anderson and V. V. Tsukruk, *Langmuir*, 2006, **23**, 265–273.
60 H. Retsos, G. Gorodyska, A. Kiriy, M. Stamm and C. Creton, *Langmuir*, 2005, **21**, 7722–7725.
61 B. Zdyrko, V. Klep, X. Li, Q. Kang, S. Minko, X. Wen and I. Luzinov, *Mater. Sci. Eng., C*, 2009, **29**, 680–684.
62 R. Sheparovych, M. Motornov and S. Minko, *Langmuir*, 2008, **24**, 13828–13832.
63 B. Zhao, W. J. Brittain, W. Zhou and S. Z. D. Cheng, *J. Am. Chem. Soc.*, 2000, **122**, 2407–2408.
64 A. M. Granville, S. G. Boyes, B. Akgun, M. D. Foster and W. J. Brittain, *Macromolecules*, 2004, **37**, 2790–2796.
65 J. Cheng, J. He, C. Li and Y. Yang, *Chem. Mater.*, 2008, **20**, 4224–4230.
66 E. Zhulina and A. C. Balazs, *Macromolecules*, 1996, **29**, 2667–2673.
67 K. L. Genson, J. Holzmueller, C. Jiang, J. Xu, J. D. Gibson, E. R. Zubarev and V. V. Tsukruk, *Langmuir*, 2006, **22**, 7011–7015.
68 I. García, A. Tercjak, N. E. Zafeiropoulos, M. Stamm and I. Mondragon, *Macromol. Rapid Commun.*, 2007, **28**, 2361–2365.
69 M. Motornov, R. Sheparovych, R. Lupitskyy, E. MacWilliams and S. Minko, *Adv. Mater.*, 2008, **20**, 200–205.
70 X. Wang, X. Xiao, X. Wang, J. Zhou, L. Li, J. Xu and B. Guo, *Macromol. Rapid Commun.*, 2007, **28**, 828–833.
71 X. Gao, S. Zhu, H. Sheardown and J. L. Brash, *Polymer*, 2010, **51**, 1771–1778.
72 L. Cheng and D. Cao, *ACS Nano*, 2011, **5**, 1102–1108.
73 M. K. Chaudhury and G. M. Whitesides, *Science*, 1992, **256**, 1539–1541.
74 K. Efimenko and J. Genzer, *Adv. Mater.*, 2001, **13**, 1560–1563.
75 B. Liedberg and P. Tengvall, *Langmuir*, 1995, **11**, 3821–3827.
76 R. H. Terrill, K. M. Balss, Y. Zhang and P. W. Bohn, *J. Am. Chem. Soc.*, 2000, **122**, 988–989.
77 S. Morgenthaler, S. Lee, S. Zürcher and N. D. Spencer, *Langmuir*, 2003, **19**, 10459–10462.
78 S.-H. Choi and B.-m. Zhang Newby, *Langmuir*, 2003, **19**, 7427–7435.
79 C. B. Ross, L. Sun and R. M. Crooks, *Langmuir*, 1993, **9**, 632–636.
80 R. R. Fuierer, R. L. Carroll, D. L. Feldheim and C. B. Gorman, *Adv. Mater.*, 2002, **14**, 154–157.
81 R. D. Piner, J. Zhu, F. Xu, S. Hong and C. A. Mirkin, *Science*, 1999, **283**, 661–663.
82 N. Ballav, A. Shaporenko, A. Terfort and M. Zharnikov, *Adv. Mater.*, 2007, **19**, 998–1000.
83 T. Wu, K. Efimenko and J. Genzer, *J. Am. Chem. Soc.*, 2002, **124**, 9394–9395.
84 T. Wu, K. Efimenko, P. Vlček, V. Šubr and J. Genzer, *Macromolecules*, 2003, **36**, 2448–2453.
85 M. Steenackers, A. Kueller, S. Stoycheva, M. Grunze and R. Jordan, *Langmuir*, 2009, **25**, 2225–2231.
86 M. R. Tomlinson and J. Genzer, *Macromolecules*, 2003, **36**, 3449–3451.
87 J. Higashi, Y. Nakayama, R. E. Marchant and T. Matsuda, *Langmuir*, 1999, **15**, 2080–2088.
88 B. P. Harris, J. K. Kutty, E. W. Fritz, C. K. Webb, K. J. L. Burg and A. T. Metters, *Langmuir*, 2006, **22**, 4467–4471.
89 C. Xu, T. Wu, C. M. Drain, J. D. Batteas and K. L. Beers, *Macromolecules*, 2005, **38**, 6–8.
90 C. Xu, T. Wu, C. M. Drain, J. D. Batteas, M. J. Fasolka and K. L. Beers, *Macromolecules*, 2006, **39**, 3359–3364.
91 L. Ionov, A. Sidorenko, M. Stamm, S. Minko, B. Zdyrko, V. Klep and I. Luzinov, *Macromolecules*, 2004, **37**, 7421–7423.
92 B. Zhao, *Langmuir*, 2004, **20**, 11748–11755.
93 M. R. Tomlinson and J. Genzer, *Langmuir*, 2005, **21**, 11552–11555.
94 X. Wang and P. W. Bohn, *Adv. Mater.*, 2007, **19**, 515–520.
95 R. R. Bhat, M. R. Tomlinson and J. Genzer, *Macromol. Rapid Commun.*, 2004, **25**, 270–274.
96 C. Schuh, S. Santer, O. Prucker and J. Ruehe, *Adv. Mater.*, 2009, **21**, 4706–4710.
97 T. Sun, G. Wang, L. Feng, B. Liu, Y. Ma, L. Jiang and D. Zhu, *Angew. Chem., Int. Ed.*, 2004, **43**, 357–360.
98 Q. He, A. Kueller, S. Schilp, F. Leisten, H.-A. Kolb, M. Grunze and J. Li, *Small*, 2007, **3**, 1860–1865.
99 J. A. Howarter and J. P. Youngblood, *Adv. Mater.*, 2007, **19**, 3838–3843.
100 S. Sanjuan and Y. Tran, *Macromolecules*, 2008, **41**, 8721–8728.
101 O. Azzaroni, B. Trappmann, P. van Rijn, F. Zhou, B. Kong and W. T. S. Huck, *Angew. Chem., Int. Ed.*, 2006, **45**, 7440–7443.
102 K. Fries, S. Samanta, S. Orski and J. Locklin, *Chem. Commun.*, 2008, 6288–6290.
103 S. Samanta and J. Locklin, *Langmuir*, 2008, **24**, 9558–9565.

104 E. Spruijt, E.-Y. Choi and W. T. S. Huck, *Langmuir*, 2008, **24**, 11253–11260.
105 D. M. Jones, J. R. Smith, W. T. S. Huck and C. Alexander, *Adv. Mater.*, 2002, **14**, 1130–1134.
106 Q. Fu, G. V. Rama Rao, S. B. Basame, D. J. Keller, K. Artyushkova, J. E. Fulghum and G. P. López, *J. Am. Chem. Soc.*, 2004, **126**, 8904–8905.
107 F. Xia, L. Feng, S. Wang, T. Sun, W. Song, W. Jiang and L. Jiang, *Adv. Mater.*, 2006, **18**, 432–436.
108 F. Xia, H. Ge, Y. Hou, T. Sun, L. Chen, G. Zhang and L. Jiang, *Adv. Mater.*, 2007, **19**, 2520–2524.
109 X. Liu, Q. Ye, B. Yu, Y. Liang, W. Liu and F. Zhou, *Langmuir*, 2010, **26**, 12377–12382.
110 N. Idota, K. Nagase, K. Tanaka, T. Okano and M. Annaka, *Langmuir*, 2010, **26**, 17781–17784.
111 N. C. Estillore, J. Y. Park and R. C. Advincula, *Macromolecules*, 2010, **43**, 6588–6598.
112 A. M. Jonas, K. Glinel, R. Oren, B. Nysten and W. T. S. Huck, *Macromolecules*, 2007, **40**, 4403–4405.
113 O. Azzaroni, A. A. Brown and W. T. S. Huck, *Angew. Chem., Int. Ed.*, 2006, **45**, 1770–1774.
114 M. T. Bernards, G. Cheng, Z. Zhang, S. Chen and S. Jiang, *Macromolecules*, 2008, **41**, 4216–4219.
115 N. D. Treat, N. Ayres, S. G. Boyes and W. J. Brittain, *Macromolecules*, 2005, **39**, 26–29.
116 A. Drechsler, A. Synytska, P. Uhlmann, M. M. Elmahdy, M. Stamm and F. Kremer, *Langmuir*, 2010, **26**, 6400–6410.
117 B. a. Lego, W. G. Skene and S. Giasson, *Macromolecules*, 2010, **43**, 4384–4393.
118 D. Li, X. Sheng and B. Zhao, *J. Am. Chem. Soc.*, 2005, **127**, 6248–6256.
119 P. Uhlmann, N. Houbenov, N. Brenner, K. Grundke, S. Burkert and M. Stamm, *Langmuir*, 2007, **23**, 57–64.
120 K. Yu, H. Wang, L. Xue and Y. Han, *Langmuir*, 2007, **23**, 1443–1452.
121 X. He, W. Yang and X. Pei, *Macromolecules*, 2008, **41**, 4615–4621.
122 T. Ishikawa, M. Kobayashi and A. Takahara, *ACS Appl. Mater. Interfaces*, 2010, **2**, 1120–1128.
123 F. Zhou and W. T. S. Huck, *Chem. Commun.*, 2005, 5999–6001.
124 T. Farhan, O. Azzaroni and W. T. S. Huck, *Soft Matter*, 2005, **1**, 66–68.
125 N. I. Abu-Lail, M. Kaholek, B. LaMattina, R. L. Clark and S. Zauscher, *Sens. Actuators, B*, 2006, **114**, 371–378.
126 F. Zhou, W. Shu, M. E. Welland and W. T. S. Huck, *J. Am. Chem. Soc.*, 2006, **128**, 5326–5327.
127 G.-G. Bumbu, M. Wolkenhauer, G. Kircher, J. S. Gutmann and R. Berger, *Langmuir*, 2007, **23**, 2203–2207.
128 F. Zhou, P. M. Biesheuvel, E.-Y. Choi, W. Shu, R. Poetes, U. Steiner and W. T. S. Huck, *Nano Lett.*, 2008, **8**, 725–730.
129 C. Li and B. C. Benicewicz, *Macromolecules*, 2005, **38**, 5929–5936.
130 T. von Werne and T. E. Patten, *J. Am. Chem. Soc.*, 1999, **121**, 7409–7410.
131 T. von Werne and T. E. Patten, *J. Am. Chem. Soc.*, 2001, **123**, 7497–7505.
132 J. Pyun, S. Jia, T. Kowalewski, G. D. Patterson and K. Matyjaszewski, *Macromolecules*, 2003, **36**, 5094–5104.
133 K. Ohno, T. Morinaga, K. Koh, Y. Tsujii and T. Fukuda, *Macromolecules*, 2005, **38**, 2137–2142.
134 D. A. Savin, J. Pyun, G. D. Patterson, T. Kowalewski and K. Matyjaszewski, *J. Polym. Sci., Part B: Polym. Phys.*, 2002, **40**, 2667–2676.
135 Y. Zhang and Z. Ye, *Macromolecules*, 2008, **41**, 6331–6338.
136 X. Wan, D. Wang and S. Liu, *Langmuir*, 2010, **26**, 15574–15579.
137 K. Ohno, K.-m. Koh, Y. Tsujii and T. Fukuda, *Macromolecules*, 2002, **35**, 8989–8993.
138 R. Jordan, N. West, A. Ulman, Y.-M. Chou and O. Nuyken, *Macromolecules*, 2001, **34**, 1606–1611.
139 M. S. Yavuz, G. C. Jensen, D. P. Penaloza, T. A. P. Seery, S. A. Pendergraph, J. F. Rusling and G. A. Sotzing, *Langmuir*, 2009, **25**, 13120–13124.
140 S. Koenig and V. Chechik, *Langmuir*, 2006, **22**, 5168–5173.
141 K. J. Watson, J. Zhu, S. T. Nguyen and C. A. Mirkin, *J. Am. Chem. Soc.*, 1998, **121**, 462–463.
142 J. Shan, M. Nuopponen, H. Jiang, T. Viitala, E. Kauppinen, K. s. Kontturi and H. Tenhu, *Macromolecules*, 2005, **38**, 2918–2926.
143 X. Fan, Q. Zhou, C. Xia, W. Cristofoli, J. Mays and R. Advincula, *Langmuir*, 2002, **18**, 4511–4518.
144 M. W. Weimer, H. Chen, E. P. Giannelis and D. Y. Sogah, *J. Am. Chem. Soc.*, 1999, **121**, 1615–1616.
145 N. S. Bell and M. Piech, *Langmuir*, 2006, **22**, 1420–1427.
146 T. Wu, G. Zou, J. Hu and S. Liu, *Chem. Mater.*, 2009, **21**, 3788–3798.
147 S. Chakraborty, S. W. Bishnoi and V. c. H. Pećrez-Luna, *J. Phys. Chem. C*, 2010, **114**, 5947–5955.
148 L. Ding, Y. Huang, Y. Zhang, J. Deng and W. Yang, *Macromolecules*, 2011, **44**, 736–743.
149 O. Schepelina and I. Zharov, *Langmuir*, 2008, **24**, 14188–14194.
150 J.-T. Sun, C.-Y. Hong and C.-Y. Pan, *J. Phys. Chem. C*, 2010, **114**, 12481–12486.
151 Z. Liu, K. Pappacena, J. Cerise, J. Kim, C. J. Durning, B. O'Shaughness and R. Levicky, *Nano Lett.*, 2002, **2**, 219–224.
152 A. Calvo, M. C. Fuertes, B. Yameen, F. J. Williams, O. Azzaroni and G. J. A. A. Soler-Illia, *Langmuir*, 2010, **26**, 5559–5567.
153 M. Mitsuishi, Y. Koishikawa, H. Tanaka, E. Sato, T. Mikayama, J. Matsui and T. Miyashita, *Langmuir*, 2007, **23**, 7472–7474.
154 I. Tokareva, S. Minko, J. H. Fendler and E. Hutter, *J. Am. Chem. Soc.*, 2004, **126**, 15950–15951.
155 S. Gupta, M. Agrawal, P. Uhlmann, F. Simon, U. Oertel and M. Stamm, *Macromolecules*, 2008, **41**, 8152–8158.
156 H. l. n. Gehan, L. Fillaud, M. M. Chehimi, J. Aubard, A. Hohenau, N. Felidj and C. Mangeney, *ACS Nano*, 2010, **4**, 6491–6500.
157 S. Gupta, M. Agrawal, P. Uhlmann, F. Simon and M. Stamm, *Chem. Mater.*, 2009, **22**, 504–509.
158 S. Diamanti, S. Arifuzzaman, J. Genzer and R. A. Vaia, *ACS Nano*, 2009, **3**, 807–818.
159 M. Mathieu, A. Friebe, S. Franzka, M. Ulbricht and N. Hartmann, *Langmuir*, 2009, **25**, 12393–12398.
160 I. S. Maeng and J. W. Park, *Langmuir*, 2003, **19**, 9973–9976.
161 U. Schmelmer, R. Jordan, W. Geyer, W. Eck, A. Golzhauser, M. Grunze and A. Ulman, *Angew. Chem., Int. Ed.*, 2003, **42**, 559–563.
162 Q. He, A. Küller, M. Grunze and J. Li, *Langmuir*, 2007, **23**, 3981–3987.
163 U. Schmelmer, A. Paul, A. Kueller, M. Steenackers, A. Ulman, M. Grunze, A. Goelzhaeuser and R. Jordan, *Small*, 2007, **3**, 459–465.
164 A. Rastogi, M. Y. Paik, M. Tanaka and C. K. Ober, *ACS Nano*, 2010, **4**, 771–780.
165 A. Rastogi, M. Y. Paik and C. K. Ober, *ACS Appl. Mater. Interfaces*, 2009, **1**, 2013–2020.
166 A. M. Jonas, Z. Hu, K. Glinel and W. T. S. Huck, *Nano Lett.*, 2008, **8**, 3819–3824.
167 Y. Ofir, I. W. Moran, C. Subramani, K. R. Carter and V. M. Rotello, *Adv. Mater.*, 2010, **22**, 3608–3614.
168 M. Kaholek, W.-K. Lee, S.-J. Ahn, H. Ma, K. C. Caster, B. LaMattina and S. Zauscher, *Chem. Mater.*, 2004, **16**, 3688–3696.
169 S. Hou, Z. Li, Q. Li and Z. F. Liu, *Appl. Surf. Sci.*, 2004, **222**, 338–345.
170 C. Slim, Y. Tran, M. M. Chehimi, N. Garraud, J.-P. Roger, C. Combellas and F. d. r. Kanoufi, *Chem. Mater.*, 2008, **20**, 6677–6685.
171 M. Kaholek, W.-K. Lee, B. LaMattina, K. C. Caster and S. Zauscher, *Nano Lett.*, 2004, **4**, 373–376.
172 M. Kaholek, W.-K. Lee, J. Feng, B. LaMattina, D. J. Dyer and S. Zauscher, *Chem. Mater.*, 2006, **18**, 3660–3664.
173 S. J. Ahn, M. Kaholek, W.-K. Lee, B. LaMattina, T. H. LaBean and S. Zauscher, *Adv. Mater.*, 2004, **16**, 2141–2145.
174 S. Morsch, W. C. E. Schofield and J. P. S. Badyal, *Langmuir*, 2010, **26**, 12342–12350.
175 M. Husemann, D. Mecerreyes, C. J. Hawker, J. L. Hedrick, R. Shah and N. L. Abbott, *Angew. Chem., Int. Ed.*, 1999, **38**, 647–649.
176 R. R. Shah, D. Merreceyes, M. Husemann, I. Rees, N. L. Abbott, C. J. Hawker and J. L. Hedrick, *Macromolecules*, 2000, **33**, 597–605.
177 N. L. Jeon, I. S. Choi, G. M. Whitesides, N. Y. Kim, P. E. Laibinis, Y. Harada, K. R. Finnie, G. S. Girolami and R. G. Nuzzo, *Appl. Phys. Lett.*, 1999, **75**, 4201–4203.
178 H. Ma, D. Li, X. Sheng, B. Zhao and A. Chilkoti, *Langmuir*, 2006, **22**, 3751–3756.
179 H.-G. Choi, J. P. Amara, T. M. Swager and K. F. Jensen, *Langmuir*, 2007, **23**, 2483–2491.

180 S. Edmondson and W. T. S. Huck, *Adv. Mater.*, 2004, **16**, 1327–1331.
181 S. Edmondson, C.-D. Vo, S. P. Armes and G.-F. Unali, *Macromolecules*, 2007, **40**, 5271–5278.
182 H. Tu, C. E. Heitzman and P. V. Braun, *Langmuir*, 2004, **20**, 8313–8320.
183 E. W. Edwards, M. F. Montague, H. H. Solak, C. J. Hawker and P. F. Nealey, *Adv. Mater.*, 2004, **16**, 1315–1319.
184 D. M. Jones and W. T. S. Huck, *Adv. Mater.*, 2001, **13**, 1256–1259.
185 T. Chen, J. Zhang, D. P. Chang, A. Garcia and S. Zauscher, *Adv. Mater.*, 2009, **21**, 1825–1829.
186 T. Chen, D. P. Chang and S. Zauscher, *Small*, 2010, **6**, 1504–1508.
187 S. Diamanti, S. Arifuzzaman, A. Elsen, J. Genzer and R. A. Vaia, *Polymer*, 2008, **49**, 3770–3779.
188 Y. Liu, V. Klep and I. Luzinov, *J. Am. Chem. Soc.*, 2006, **128**, 8106–8107.
189 B. Zdyrko, O. Hoy, M. K. Kinnan, G. Chumanov and I. Luzinov, *Soft Matter*, 2008, **4**, 2213–2219.
190 T. A. von Werne, D. S. Germack, E. C. Hagberg, V. V. Sheares, C. J. Hawker and K. R. Carter, *J. Am. Chem. Soc.*, 2003, **125**, 3831–3838.
191 M. Beinhoff, A. T. Appapillai, L. D. Underwood, J. E. Frommer and K. R. Carter, *Langmuir*, 2006, **22**, 2411–2414.
192 S. B. Jhaveri, M. Beinhoff, C. J. Hawker, K. R. Carter and D. Y. Sogah, *ACS Nano*, 2008, **2**, 719–727.
193 F. J. Xu, Y. Song, Z. P. Cheng, X. L. Zhu, C. X. Zhu, E. T. Kang and K. G. Neoh, *Macromolecules*, 2005, **38**, 6254–6258.
194 O. Prucker, J. Habicht, I.-J. Park and J. Rühe, *Mater. Sci. Eng., C*, 1999, **8-9**, 291–297.
195 F. Zhou, L. Jiang, W. Liu and Q. Xue, *Macromol. Rapid Commun.*, 2004, **25**, 1979–1983.
196 F. Zhou, Z. Zheng, B. Yu, W. Liu and W. T. S. Huck, *J. Am. Chem. Soc.*, 2006, **128**, 16253–16258.
197 G. L. Li, D. Wan, K. G. Neoh and E. T. Kang, *Macromolecules*, 2010, **43**, 10275–10282.
198 R. Dong, R. P. Molloy, M. Lindau and C. K. Ober, *Biomacromolecules*, 2010, **11**, 2027–2032.
199 R. M. Hensarling, V. A. Doughty, J. W. Chan and D. L. Patton, *J. Am. Chem. Soc.*, 2009, **131**, 14673–14675.
200 S. V. Orski, A. A. Poloukhtine, S. Arumugam, L. Mao, V. V. Popik and J. Locklin, *J. Am. Chem. Soc.*, 2010, **132**, 11024–11026.
201 G. Zotti, S. Zecchin, B. Vercelli, A. Berlin, S. Grimoldi, L. Groenendaal, R. Bertoncello and M. Natali, *Chem. Mater.*, 2004, **17**, 3681–3694.
202 I. W. Moran, S. B. Jhaveri and K. R. Carter, *Small*, 2008, **4**, 1176–1182.
203 N. Khanduyeva, V. Senkovskyy, T. Beryozkina, M. Horecha, M. Stamm, C. Uhrich, M. Riede, K. Leo and A. Kiriy, *J. Am. Chem. Soc.*, 2008, **131**, 153–161.
204 V. Senkovskyy, R. Tkachov, T. Beryozkina, H. Komber, U. Oertel, M. Horecha, V. Bocharova, M. Stamm, S. A. Gevorgyan, F. C. Krebs and A. Kiriy, *J. Am. Chem. Soc.*, 2009, **131**, 16445–16453.
205 T. Beryozkina, K. Boyko, N. Khanduyeva, V. Senkovskyy, M. Horecha, U. Oertel, F. Simon, M. Stamm and A. Kiriy, *Angew. Chem., Int. Ed.*, 2009, **48**, 2695–2698.
206 R. M. Hensarling, S. B. Rahane, A. P. LeBlanc, B. J. Sparks, E. M. White, J. Locklin and D. L. Patton, *Polym. Chem.*, 2011, **2**, 88–90.
207 S. G. Im, K. W. Bong, B.-S. Kim, S. H. Baxamusa, P. T. Hammond, P. S. Doyle and K. K. Gleason, *J. Am. Chem. Soc.*, 2008, **130**, 14424–14425.